Synchrotron radiation X-ray fluorescence analysis of Fe, Zn and Cu in mice brain associated with Parkinson's disease[*]

TIAN Tian (田甜),[1,2,3] ZHANG Ji-Chao (张继超),[1,2] LEI Hao-Zhi (雷豪志),[1,2] ZHU Ying (诸颖),[1,2] SHI Ji-Ye (施继晔),[4]
HU Jun (胡钧),[1,2] HUANG Qing (黄庆),[1,2] FAN Chun-Hai (樊春海),[1,2] and SUN Yan-Hong (孙艳红)[1,2,†]

[1]*Key Laboratory of Interfacial Physics and Technology,*
Chinese Academy of Sciences, Shanghai 201800, China
[2]*Shanghai Institute of Applied Physics, Chinese Academy of Sciences, Shanghai 201800, China*
[3]*University of Chinese Academy of Sciences, Beijing 100049, China*
[4]*UCB Pharm, Slough SL1 3WE, UK*

The contents and distributions of metal elements in the brain are closely related to neurodegenerative diseases. In this study, we examined Fe, Cu and Zn contents in the brain section associated with Parkinson's disease (PD) using synchrotron radiation X-ray fluorescence (SRXRF). PD mouse model induced by 1-methyl-4-phenyl-1,2,3,6-terahydropyridine (MPTP) was used for the elemental analysis (e.g., Fe, Cu and Zn) in the substantia nigra pars compacta (SNpc) region of mice brain tissue samples. We found that mice in the MPTP group had higher contents of Fe, Cu and Zn in the SNpc than the control group. After treating the PD mice with rapamycin, the contents of Fe, Cu and Zn were reduced, the dopamine neurons and motor function were rescued correspondingly. The results prompted that the SRXRF provided an ideal method for tracing and analyzing the metal elements in the brain section to assess the pathological changes of PD model and the therapeutic effect of drugs.

Keywords: Synchrotron radiation X-ray fluorescence, Metal element, Trace and analysis, Rapamycin, Parkinson's diseases

I. INTRODUCTION

Parkinson's disease (PD) is a progressive neurodegenerative disorder mainly characterized by the loss of dopaminergic neurons from the substantia nigra pars compacta (SNpc) and the presence of the Lewy bodies [1]. Oxidative stress is an important pathogenic factors in PD [2, 3]. Postmortem studies showed that oxidative stress induced neurons death and the level of related oxidative stress marker was higher in PD patients [4]. Endogenous metal elements are essential requirement and subject to complex regulation in biological systems. Excessive metal elements cause oxidative stress *in vivo* [4]. It was reported that Cu and Zn contents in cerebrospinal fluid of PD patients were higher than those of healthy persons [5, 6]. This indicates that the disturbance of metal homeostasis in biological environment may have high association with PD. Elemental mapping of metals is therefore of primary importance to reveal their pathological roles in the disease development.

Among the methods of elemental mapping in biological samples, X-ray fluorescence analysis (XRF) and laser ablation inductively coupled plasma mass spectrometry (LA-ICP/MS) are highly specific and sensitive methods for identification and distribution analysis of metals and nonmetals in cell or tissue [7–11]. Matusch A *et al*. [12] used the LA-ICP/MS for mapping Cu, Mn, Fe and Zn in brains of Parkinsonism mouse model and affirmed the role of Cu availability in PD. As a nondestructive multielemental analytical technique [10, 13, 14], XRF can be used for imaging of trace elements in biological samples, with a spatial resolution of sub-mm and limit of detection (LOD) of several mg/g. With advances of third generation synchrotron radiation (SR) sources, Synchrotron radiation X-ray fluorescence (SRXRF) is a nondestructive multi- elemental analysis technique with higher spatial resolution (sub-μm) and higher sensitivity (LODs of 50–100 ng/g for many elements) [14–16]. Using SRXRF, Wang *et al*. [17] studied distributions of metal elements in the brain section of a transgenic mouse model of Alzheimer's disease(AD), and developed a method for mapping trace elements in sections of bio-tissues; Korbas *et al*. [18] observed organomercury uptake and accumulation in tissue and cells of zebrafish larvae; and Zhang *et al*. [19] presented a bioprobe based on dendrimer-folate-copper conjugates, and found that the metal nanoclusters within dendrimer exhibited excellent tumor-targeting properties in human mouth epidermal carcinoma KB cells. SRXRF elemental mapping was also used to study cytotoxicity of nano particles, such as TiO$_2$ and quantum dots [20, 21].

Abnormal brain contents and distributions of metal elements are closely related to PD. SRXRF offers unique opportunities to non-destructively visualize the distributions of metal elements and determine metal contents in brain tissue samples. In this study, contents and distributions of Fe, Cu and Zn in the SNpc of PD mouse brain were determined using SRXRF. The PD mice model was induced by 1-methyl-4-phenyl-1,2,3,6-terahydropyridine (MPTP) injection. Rapymycin, a protector of neurons against MPTP [22],

[†] Corresponding author, sunyanhong@sinap.ac.cn

was used to treat PD mice for 12 days. The elemental mapping study is to explore pathological roles of metals in PD and therapeutic effect of drugs.

II. MATERIALS AND METHODS

A. Ethics statement for the animal experiments

This study was conducted in strict accordance with recommendations of the Guidelines for Animal Care and Use, Shanghai Laboratory Animal Center, Chinese Academy of Sciences. The animal protocols were approved by Committee on Ethics of Animal Experiments of Shanghai University of Traditional Chinese Medicine.

B. Animals

Male C57BL/6J mice, weighing (24 ± 2) g, were obtained from Shanghai Laboratory Animal Center, Chinese Academy of Sciences and housed in the animal center of Shanghai University of Traditional Chinese Medicine. The breeding room $((22 \pm 2)\,°C$, 60%–80% humidity) was illuminated by an artificial light cycle of 12-h light and 12-h darkness every day, and disinfected regularly.

C. MPTP and Rapamycin treatment

The mice were randomly assigned to three groups: control, MPTP (1-methyl-4-phenyl-1,2,3,6-terahydropyridine) and MPTP with rapamycin treatment (M + Rapa). The MPTP and M + Rapa groups received one intraperitoneal injection of MPTP-HCl per day (30 mg/kg free base; Sigma, USA) for five consecutive days [23]. The control group was injected with physiological saline solution (0.9% NaCl). The M + Rapa group received one intraperitoneal injection with rapamycin per day 30 min before MPTP injection. The daily doses of rapamycin were 10 mg/kg/d in the first two days and 5 mg/kg/d from Day 3 to Day 12. Rapamycin was dissolved in saline adding 4% ethanol, 1% tween-80 and 5% polyethylene glycol 400.

D. Behavioral test

On Day 11 after rapamycin injection, the rotarod instrument was used to test the exercise performance of mice in each group. The overall rod performance (ORP) method was used, as described by Rozas *et al*. [24]. Before testing, mice were trained on the machine at an accelerating speed. After testing was performed, time of mice staying on the rod was recorded at successive rotational speeds of 10, 15, 20, 25 and 30 rpm, for a maximum of 300 s at each speed. At the end, the ORP score for each mouse was calculated by the trapezoidal method [25].

E. Immunohistochemistry

After the 12-day rapamycin injection, the mice were perfused transcardially with 4% paraformaldehyde in 0.1 M phosphate buffer after anaesthesia. The removed substantia nigra was immersed overnight in 4% paraformaldehyde. For immunohistochemical staining, the paraffin sections cut at 5 μm thickness through the entire SNpc were dewaxed, and immersed in boiling solution (0.01 M sodium citrate buffer) for 30 min for antigen retrieval. After antigen retrieval, the sections were incubated with 3% H_2O_2 (diluted in methanol) for 10 min. Next, the sections were incubated with 6% bovine serum albumin (BSA) for 30 min at room temperature, and then with rabbit tyrosine hydroxylase antibody (TH, 1:500; Abcam) overnight at 4 °C. The next day, the sections were incubated with biotinylated anti-rabbit IgG for 30 min at 37 °C, and then with horse radish peroxidase (HRP) for 10 min. Then, the sections were incubated with 3,3'-diaminobenzidine (DAB) for 3 min (Histostain-Plus IHC Kit, MiaoTong). Finally, the sections were dehydrated and covered, and imaged by a bright-field microscope. We selected five consecutive sections at the same anatomical position from one sample to count the TH-positive cells in the SNpc.

F. Western Blotting

Brain tissues of the rapamycin-injected mice were removed and the SNpc were dissected quickly on ice. The tissues were homogenized in protein lysis buffer, which was composed of 150 mM NaCl, 5 mM EDTA, 50 mM Tris-HCl (pH 7.0), 1% Nonidet P-40, 1% sodium dodecyl sulfonate (SDS) and Mini mixture protease inhibitors (Roche Diagnostics). The protein concentration was measured using the bicinchoninic acid (B-CA) protein assay kit (Thermo Scientific). The protein were boiled with loading buffer at 95 °C for 5 min, subpackaged into eppendorf (EP) tube, and stored at −80 °C. In this study, 4%–10% SDS-polyacrylamide gel was used to separate the protein samples. After blocking for 1 h in 5% nonfat milk (dry milk dissolved into 0.1 M phosphate buffer with 0.1% Tween-20, the diluent named PBST), the polyvinylidene fluoride (PVDF) membranes were incubated overnight at 4 °C with a primary antibody (TH, rabbit, 1:1000, Millipore). The next day, PVDF membranes were washed using PBST for 30 min, and incubated with an HRP-conjugated anti-rabbit antibody (1:10 000, Sigma) at room temperature for 1 h. After 30-min washing, enhanced chemiluminescent (ECL) kit (Millipore) was used to incubate with membranes for 30 s, and characterized by Gel & Blot Imaging system (Syngene). The band intensities of the proteins were quantified using the Quantity One software (Bio-Rad).

G. Transmission electron microscopy

The mice were perfused transcardially with 4% paraformaldehyde and 1% glutaraldehyde in 0.1 M phosphate buffer. The removed substantia nigra was immersed in 2.5%

glutaraldehyde for 2 h. The sections of 100 μm thick were cut using a vibratome (Leica), and then fixed in 1% osmium tetroxide for 1 h. The temperature was controlled at 4 °C. The sections were dehydrated, and embedded in epoxy resin, then cut into 70 nm thickness. Finally, the sections were stained with 5% uranyl acetate, and analyzed using TEM.

H.   SRXRF image and data analysis

For SRXRF imaging, the brain tissues were removed and postfixed in 4% paraformaldehyde for 2 h, and then immersed in 30% sucrose overnight at 4 °C. The tissues were sectioned at 50 μm using a vibratome (Leica), the sections were collected through the entire substantia nigra. Samples were fixed on 3 μm thick Mylar films.

Samples were analyzed on the hard X-ray microprobe beamline (BL15U1) at Shanghai Synchrotron Radiation Facility (SSRF) [26]. Si(111) double crystal was used to monochromatize the X-rays to 10 keV, so as to excite the Kα fluorescence of Fe, Cu and Zn. The X-ray beam spot was adjusted to 100 μm × 100 μm by narrow slits. The samples were placed at 45° to the beam incidence. SRXRF spectra were collected with a 50 mm^2 silicon-drift detector (Vortex, USA) placed at 90° to the beam incidence. All samples were placed on a 7-axis platform with a high spatial resolution and monitored by a PC-connected microscope. The samples were raster-scanned in 100-μm steps in the x and z directions. The dwell time was 1 second per pixel and about 2 h for the whole section.
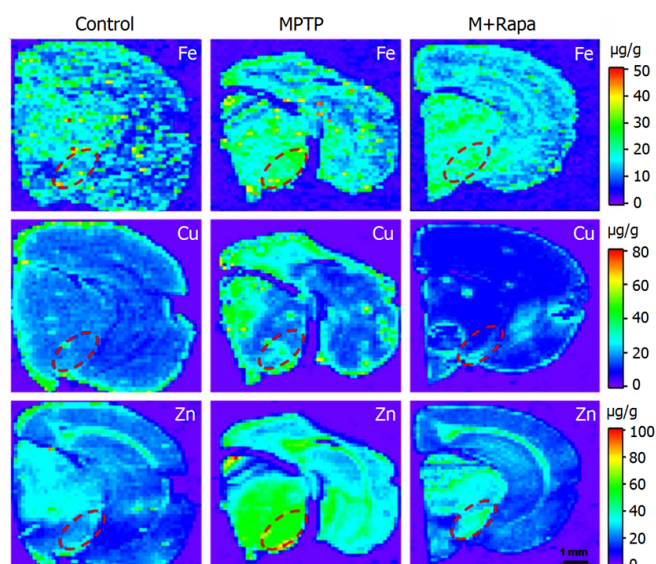

Fig. 1. (Color online) Elemental mapping of Fe, Cu and Zn in brain slices of the mouse groups. The region in the red ellipse is the SNpc region.

PyMCA toolkit was used to fit the SRXRF spectra [27]. The Compton scattering in a spectrum was used as internal standard to compensate the differences in density and thick-

ness of thin tissue sections [28, 29]. Standard reference materials of bovine liver (NIST 1577a) were sandwiched between two Mylar films, and trace elements in glass (NIST 612) were linearly scanned under the same experimental conditions as the brain sections. Fe, Cu and Zn contents in the samples were obtained through the normalization to Compton scattering intensity and the ratios of Compton intensity against the known concentrations of each element in the standard reference materials. Finally, plot2d.py software was used to obtain 2D elemental maps with false color based on the elemental contents. As a python 2D graphic software for ASCII/MDA File, plot2d.py can extract both 2D array from ASCII text file and multiple 2D image arrays from MDA 2D/3D scan file. Selected SNpc regions of brain slices were used to calculate the average contents of metal elements.

I.   Statistical analysis

The Graph Pad Prism software (v5.0) was used for all statistics analysis. All data are presented as mean ± standard error. Differences among the experimental groups were performed using a Student t test. In all analyses, statistical significance was considered at $P < 0.05$.
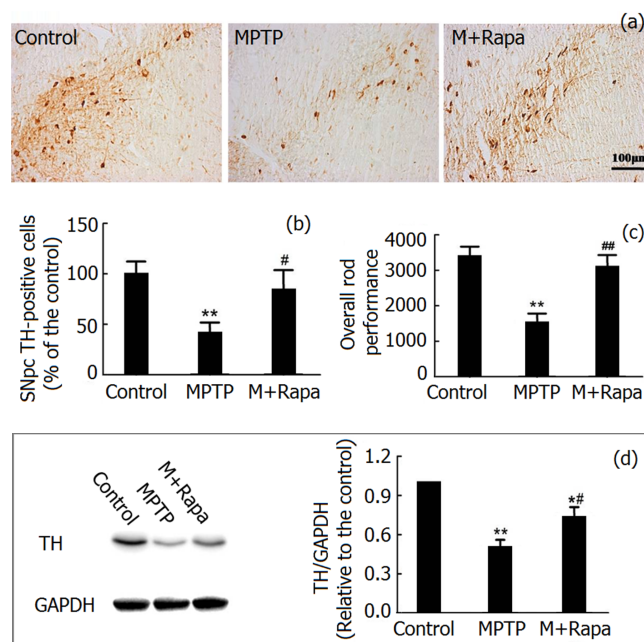

Fig. 2. (Color online) Rapamycin improved exercise performance and protected dopamine neurons in MPTP-treated mice-TH-positive neurons in the SNpc in a high magnification optical image (a), the counts of TH-positive neurons in the SNpc of each group (b, $n = 4$ or 5), ORP scores of each group (c, $n = 10$), and TH immunoblot levels in the SNpc of mice in each group (d). **$P < 0.01$,*$P < 0.05$ compared with the control group. #$P < 0.05$, ##$P < 0.01$ compared with the MPTP group.
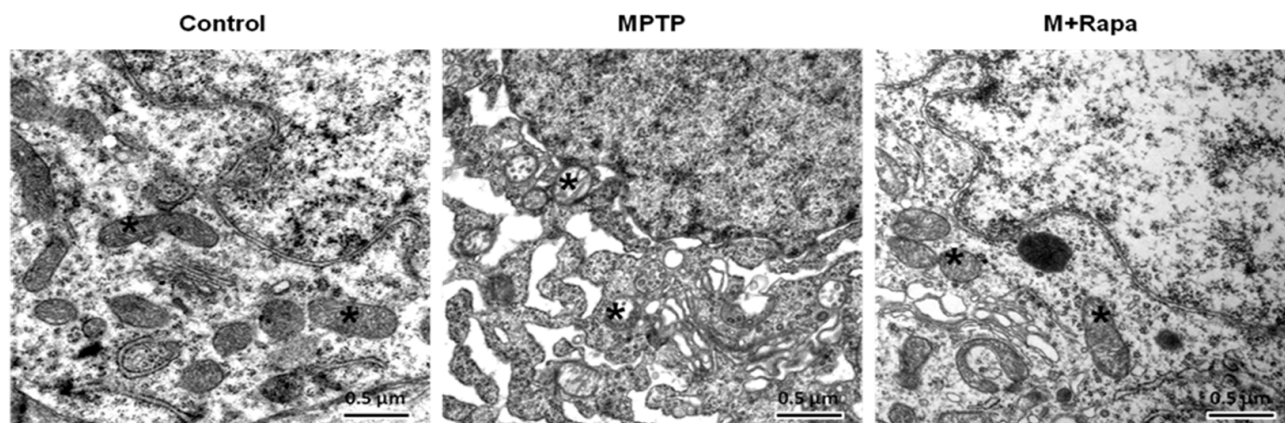
Fig. 3. TEM images of mitochondrial ultrastructure. Mitochondria in the control group were normal. Mitochondria in the MPTP group were swollen. Mitochondria in the M + Rapa group turned to be normal (asterisk, mitochondria).

III. RESULTS

SRXRF was used for elemental analysis of the brain samples of each mouse. SNpc is the primary region associated with PD. Slices of half brain included SNpc were investigated. Elemental distributions of Fe, Cu and Zn in the brain slices were obtained (Fig. 1). The Fe contents range from 5 to 15 µg/g in most of the brain regions. However, significant accumulation of Fe, up to 26 µg/g, was found in the SNpc of PD mice, being significantly higher than the control group (16 µg/g). Cu was found to accumulate in the cerebral cortex, superior colliculus and SNpc of PD mice, and the Cu content in SNpc (21 µg/g) was obviously higher than that in the control group (14 µg/g). Images of Zn exhibited notable accumulation in the cerebral cortex and hippocampus. The Zn content in the SNpc of PD mice was about 60 µg/g, much higher than that (30 µg/g) in the control group. After treatment with rapamycin for 12 days, Fe, Cu and Zn contents in the SNpc of brain section were reduced to 20, 14 and 38 µg/g, respectively, suggesting that rapamycin could regulate the metal homeostasis in the SNpc region of PD mouse brain.

The number of dopamine neurons and motor function of mice in each group were examined. In the MPTP group, the number of TH-positive cells and the expression of TH protein in the SNpc of mouse brain was about 50% lower than the control group, and the ORP scores which reflected motor function declined remarkably ($P < 0.01$, Fig. 2) After rapamycin treatment, the M + Rapa group showed obviously higher ORP scores than the MPTP group ($P < 0.01$, Fig. 2(c)). The number of TH-positive cells in SNpc of the M + Rapa group was more than that of MPTP group ($P < 0.01$, Fig. 2(a), 2(b)). Also, the expression of TH protein in the SNpc of the M + Rapa group is higher than that of MPTP group ($P < 0.05$, Fig. 2(d)).

Transmission electron microscopy (TEM) was used to verify the potential mechanism of rapamycin treated on PD mice (Fig. 3). The mitochondrion of the MPTP group exhibited a loss of matrix density, swelling and cristae disruption. This is a characteristic of oxidative damages. After rapamycin treatment, the structure of mitochondrion was rescued significantly.

IV. DISCUSSION

Transition metal elements like Fe, Cu and Zn are important in regulating neuronal activity. The changes in contents and distributions of metal elements are closely related to neurodegenerative disorder, such as AD and PD [30–32]. It was reported that Cu and Zn contents in cerebrospinal fluid of PD patients were higher than those of healthy people [5, 6]. Other studies showed that chronic exposure to copper was associated with PD [33–36]. SRXRF offered unique opportunities to non-destructively visualize the metal elements distributions in brain tissue or neuron cells [37–39]. We used SRXRF to examine the metal elements distributions in the SNpc of mouse brain section. The results show that Fe, Cu and Zn contents of the MPTP group are higher than those of the control group.

Among these metals, the redox-active Fe and Cu, are associated with the generation of reactive oxygen species (ROS). They can induce ROS generation from the Fenton reaction [34]. Meanwhile, imbalance of Cu can cause mitochondria dysfunction [40]. Unlike Fe and Cu, Zn is not a redox-active metal, but it can also induce oxidative stress [41, 42]. In cells, increased content of free Zn is highly cytotoxic. In this study, we found the increased contents of Fe, Cu and Zn and the destroyed structures of mitochondria in MPTP treated mice. Also we found that the number of TH-positive cells, expression of TH protein and the ORP scores declined remarkably in MPTP treated mice. These imply that Fe, Cu and Zn involved in the oxidative damages of the neuron cells were induced by MPTP.

Rapamycin, an inhibitor of m-TOR, was reported to have neuroprotective effect on dopamine neurons in MPTP- induced PD mice model. Most studies explained the protective effect of rapamycin by activating autophagy [43, 44], while few studies focused on metal elements homeostasis. Here,

we observed that rapamycin protected dopamine neurons against MPTP. This is similar to previous researches. Interestingly, we found that Fe, Cu and Zn contents in the SNpc area of mice brain slices were reduced after treatment with rapamycin. Correspondingly, the TH-positive cells and mitochondria structures in the SNpc area of mice brain were restored, and the exercise performance was improved remarkably after rapamycin treatment. The results indicate that the effect of rapamycin on MPTP-treated mice could be related with metal homeostasis regulation.

creased significantly in the MPTP treated mice. These metal elements are associated with production of ROS, which are closely related to PD [18]. Rapamycin could reduce the contents of these metals, thereby the impairment of the dopamine neurons and the motor functions can be restored. SRXRF provided an ideal imaging method for biological tissue samples to reveal the pathological mechanisms of metals homeostasis in PD mice. In addition, the study also prompted that the protective effect of rapamycin in the MPTP-induced mouse possibly related with its regulating effect on the metal imbalance of the brain.

V.   CONCLUSION

In summary, we obtained the distributions and contents of metal elements in the SNpc of the mice brain slice by using the SRXRF. We found that the contents of Fe, Cu and Zn in-

ACKNOWLEDGMENTS

[1] Sherer T B and Greenamyre J T. Oxidative damage in Parkinson's disease. Antioxid Redox Signal, 2005, **7**: 627–629. DOI: 10.1089/ars.2005.7.627

[2] Jenner P and Olanow C W. Understanding cell death in Parkinson's disease. Ann Neurol, 1998, **44**: S72–S84. DOI: 10.1002/ana.410440712

[3] Uttara B, Singh A V, Zamboni P, *et al*. Oxidative stress and neurodegenerative diseases: a review of upstream and downstream antioxidant therapeutic options. Curr Neuropharmacol, 2009, **7**: 65–74. DOI: 10.2174/157015909787602823

[4] Jenner P. Oxidative stress in Parkinson's disease. Ann Neurol, 2003, **53**: S26–S38. DOI: 10.1002/ana.10483

[5] Jomova K, Vondrakova D, Lawson M, *et al*. Metals, oxidative stress and neurodegenerative disorders. Mol Cell Biochem, 2010, **345**: 91–104. DOI: 10.1007/s11010-010-0563-x

[6] Hozumi I, Hasegawa T, Honda A, *et al*. Patterns of levels of biological metals in CSF differ among neurodegenerative diseases. J Neurol Sci, 2011, **303**: 95–99. DOI: 10.1016/j.jns.2011.01.003

[7] Ogunrin A O, Komolafe M A, Sanya E O, *et al*. Trace metals in patients with Parkinson's disease: a multi-center case-control study of nigerian patients. J Neurol Epidemiol, 2013, **1**: 31–38. DOI: 10.12974/2309-6179.2013.01.01.4

[8] Szczerbowska-Boruchwska M, Lankosz M, Ostachowicz J, *et al*. Topographic and quantitative microanalysis of human central nervous system tissue using synchrotron radiation. X-ray Spectrum, 2004, **33**: 3–11. DOI: 10.1002/xrs.674

[9] Ralle M and Lutsenko S. Quantitative imaging of metals in tissues. BioMetals, 2009, **22**: 197–205. DOI: 10.1007/s10534-008-9200-5

[10] Lobinski R, Moulin C and Ortega R. Imaging and speciation of trace elements in biological environment. Biochimie, 2006, **88**: 1591-1604. DOI: 10.1016/j.biochi.2006.10.003

[11] Li X Y, Takahiro S, Ishii Y, *et al*. External micro-PIXE analysis of Nd^{3+} accumulation in Euglena gracilis. Nucl Sci Tech, 2014, **25**: 040201. DOI: 10.13538/j.1001-8042/nst.25.040201

[12] Matusch A, Depboylu C, Palm C, *et al*. Cerebral bioimaging of Cu, Fe, Zn, and Mn in the MPTP mouse model of Parkinson's disease using laser ablation inductively coupled plasma mass spectrometry (LA-ICP-MS). J Am Soc Mass Spectr, 2010, **21**:

161–171. DOI: 10.1016/j.jasms.2009.09.022

[13] Wang J, Liu M Z, Tuo X G, *et al*. A genetic-algorithm-based neural network approach for EDXRF analysis. Nucl Sci Tech, 2014, **25**: 0302031. DOI: 10.13538/j.1001-8042/nst.25.030203

[14] Popescu B F G, George M J, Bergmann U, *et al*. Mapping metals in Parkinson's and normal brain using rapid-scanning X-ray fluorescence. Phys Med Biol, 2009, **54**: 651–663. DOI: 10.1088/0031-9155/54/3/012

[15] Popescu B F G, Robinson C A, Chapman L D, *et al*. Synchrotron X-ray fluorescence reveals abnormal metal distributions in brain and spinal cord in spinocerebellar ataxia: a case report. Cerebellum, 2009, **8**: 340–351. DOI: 10.1007/s12311-009-0102-z

[16] Qin Y, Fan C H, Huang Q, *et al*. Applications of large-scale scientific radiation light source in analytical chemistry for life science. Scientia Sinica Chimica, 2010, **40**: 22–30. (in Chinese)

[17] Wang H J, Wang M, Wang B, *et al*. Quantitative imaging of element spatial distribution in the brain section of a mouse model of Alzheimer's disease using synchrotron radiation X-ray fluorescence analysis. J Anal Atom Spectrom, 2010, **25**: 328–333. DOI: 10.1039/B921201A

[18] Korbas M, Blechinger S R, Krone P H, *et al*. Localizing organomercury uptake and accumulation in zebrafish larvae at the tissue and cellular level. P Natl Acad Sci USA, 2008, **105**, 12108–12112. DOI: 10.1073/pnas.0803147105

[19] Zhang Y Q, Xu X P, Wang L, *et al*. Dendrimer-folate-copper conjugates as bioprobes for synchrotron X-ray fluorescence imaging. Chem Commun, 2013, **49**: 10388–10390. DOI: 10.1039/c3cc46057f

[20] Zhu Y, Cai X Q, Li J, *et al*. Synchrotron-based X-ray microscopic studies for bioeffects of nanomaterials. Nanomedicine, 2014, **10**: 515–524. DOI: 10.1016/j.nano.2013.11.005

[21] Chen N, He Y, Su Y Y, *et al*. The cytotoxicity of cadmium-based quantum dots. Biomaterials, 2012, **33**: 1238–11244. DOI: 10.1016/j.biomaterials.2011.10.070

[22] Dehay B, Bové J, Rodriguez-Muela N, *et al*. Pathogenic lysosomal depletion in Parkinson's disease. J Neurosci, 2010, **30**: 12535–12544. DOI: 10.1523/JNEUROSCI.1920-10.2010

[23] Jackson-Lewis V and Przedborski S. Protocol for the MPTP mouse model of Parkinson's disease. Nat Protoc, 2007, **2**: 141–151. DOI: 10.1038/nprot.2006.342

[24] Rozas G, López-Martin E, Guerra M J, *et al*. The overall rod performance test in the MPTP-treated-mouse model of Parkinsonism. J Neurosci Meth, 1998, **83**: 165–175. DOI: 10.1016/S0165-0270(98)00078-8

[25] Rozas G, Guerra M J and Labandeira-Garcia J L. An automated rotarod method for quantitative drug-free evaluation of overall motor deficits in rat models of parkinsonism. Brain Res Protoc, 1997, **2**: 75–84. DOI: 10.1016/S1385-299X(97)00034-2

[26] Zhang J C, Li B, Zhang Y, *et al*. Synchrotron radiation X-ray fluorescence analysis of biodistribution and pulmonary toxicity of nanoscale titanium dioxide in mice. Analyst, 2013, **138**: 6511–6516. DOI: 10.1039/c3an01267k

[27] Solé V A, Papillon E, Cotte M, *et al*. A multiplatform code for the analysis of energy-dispersive X-ray fluorescence spectra. Spectrochim Acta B, 2007, **62**: 63–68. DOI: 10.1016/j.sab.2006.12.002

[28] Vekemans B, Vincze L, Somogyi A, *et al*. Quantitative X-ray fluorescence analysis at the ESRF ID18F microprobe. Nucl Instrum Meth B, 2003, **199**: 396–401. DOI: 10.1016/S0168-583X(02)01396-4

[29] Janssens K, De Nolf W, Van Der Snickt G, *et al*. Recent trends in quantitative aspects of microscopic X-ray fluorescence analysis. Trac-trend Anal Chem, 2010, **29**: 464–478. DOI: 10.1016/j.trac.2010.03.003

[30] Bush A I. Metals and neuroscience. Curr Op Chem Biol, 2000, **4**: 184–191. DOI: 10.1016/S1367-5931(99)00073-3

[31] Popescu B F G, Robinson C A, Rajput A, *et al*. Iron, copper, and zinc distribution of the cerebellum. Cerebellum, 2009, **8**: 74–79. DOI: 10.1007/s12311-008-0091-3

[32] Paris I, Dagnino-Subiabre A, Marcelain K, *et al*. Copper neurotoxicity is dependent on dopamine-mediated copper uptake and one-electron reduction of aminochrome in a rat substantia nigra neuronal cell line. J Neurochem, 2001, **77**: 519–529. DOI: 10.1046/j.1471-4159.2001.00243.x

[33] Gorell J M, Johnson C C, Rybicki B A, *et al*. Occupational exposure to manganese, copper, lead, iron, mercury and zinc and the risk of Parkinson's disease. Neurotoxicology, 1999, **20**: 239–247.

[34] Prousek J. Fenton chemistry in biology and medicine. Pure Appl Chem, 2007, **79**: 2325–2338.

[35] Ide-Ektessabi A, Fujisawa S and Yoshida S. Chemical state imaging of iron in nerve cells from a patient with Parkinsonism-dementia complex. J Appl Phys, 2002, **91**: 1613–1617. DOI: 10.1063/1.1426244

[36] Davies K M, Bohic S, Carmona A, *et al*. Copper pathology in vulnerable brain regions in Parkinson's disease. Neurobiol Aging, 2014, **35**: 858–866. DOI: 10.1016/j.neurobiolaging.2013.09.034

[37] Popescu B F G and Nichol H. Mapping brain metals to evaluate therapies for neurodegenerative disease. CNS Neurosci Ther, 2011, **17**: 256–268. DOI: 10.1111/j.1755-5949.2010.00149.x

[38] Ide-Ektessabi A and Rabionet M. The role of trace metallic elements in neurodegenerative disorders: Quantitative analysis using XRF and XANES spectroscopy. Anal Sci, 2005, **21**: 885–892. DOI: 10.2116/analsci.21.885

[39] Miller L M, Wang Q, Telivala T P, *et al*. Synchrotron-based infrared and X-ray imaging shows focalized accumulation of Cu and Zn co-localized with β-amyloid deposits in Alzheimer's disease. J Struct Biol, 2006, **155**: 30–37. DOI: 10.1016/j.jsb.2005.09.004

[40] Rossi L, Lombardo M F, Ciriolo M R, *et al*. Mitochondrial dysfunction in neurodegenerative diseases associated with copper imbalance. Neurochem Res, 2004, **29**: 493–504. DOI: 10.1023/B:NERE.0000014820.99232.8a

[41] Lee S J and Koh J Y. Roles of zinc and metallothionein-3 in oxidative stress-induced lysosomal dysfunction, cell death, and autophagy in neurons and astrocytes. Molecular Brain, 2010, **3**: 30. DOI: 10.1186/1756-6606-3-30

[42] Gilgun-Sherki Y, Melamed E and Offen D. Oxidative stress induced-neurodegenerative diseases: the need for antioxidants that penetrate the blood brain barrier. Neuropharmacology, 2001, **40**: 959–975. DOI: 10.1016/S0028-3908(01)00019-3

[43] Malagelada C, Jin Z H, Jackson-Lewis V, *et al*. Rapamycin protects against neuron death in *in vitro* and *in vivo* models of Parkinson's disease. J Neurosci, 2010, **30**: 1166–1175. DOI: 10.1523/JNEUROSCI.3944-09.2010

[44] Jiang J H, Jiang J A, Zuo Y Y, *et al*. Rapamycin protects the mitochondria against oxidative stress and apoptosis in a rat model of Parkinson's disease. Int J Mol Med, 2013, **31**: 825–832. DOI: 10.3892/ijmm.2013.1280